small
NANO MICRO
www.small-journal.com

On-Skin Triboelectric Nanogenerator and Self-Powered Sensor with Ultrathin Thickness and High Stretchability

*Xiangyu Chen, Yali Wu, Jiajia Shao, Tao Jiang, Aifang Yu, Liang Xu, and Zhong Lin Wang**

Researchers have devoted a lot of efforts on pursuing light weight and high flexibility for the wearable electronics, which also requires the related energy harvesting devices to have ultrathin thickness and high stretchability. Hence, an elastic triboelectric nanogenerator (TENG) is proposed that can serve as the second skin on human body. The total thickness of this TENG is about 102 μm and the device can work durably under a strain of 100%. The carbon grease is painted on the surface of elastomer film to work as stretchable electrode and thus the fine geometry control of the electrode can be achieved. This elastic TENG can even work on the human fingers without disturbing body movement. The open-circuit voltage and short-circuit current from the device with a contact area of 9 cm^2 can reach 115 V and 3 μA, respectively. Two kinds of self-powered sensor systems with optimized identification strategies are also designed to demonstrate the application possibility of this elastic TENG. The superior characteristics of ultrathin thickness, high stretchability, and fine geometry control of this TENG can promote many potential applications in the field of wearable self-powered sensory system, electronics skin, artificial muscles, and soft robotics.

1. Introduction

With the rapid development of flexible and stretchable electronics, the mechanical compliance and biocompatibility of the electronic devices have been significantly enhanced and a series of novel conductive materials or semiconductors with excellent stretchability have also been discovered.[1,2] All of these progresses have strongly stimulated the people's desires for portable, wearable, and even implantable electronic system, such as flexible display, wearable sensory system, for health monitoring, interactive electronics, and so on.[3–5] For all these portable or wearable electronic devices, a sustainable and highly stretchable power supplier with light weight, shape-adaptability, and environmental friendliness would be of great help for the real applications of these devices. A promising approach to satisfy these requirements is to directly power electronic system by collecting energy from the ambient environment, which brings a concept of self-powered nanosystems.[6,7] In the past few years, triboelectric nanogenerator (TENG), which can directly convert various mechanical motions into electrical energy, has been served as the energy supplier for many electronic and sensory systems to realize all sorts of functions.[8–10] TENG device has the strong adaptability, high flexibility and good environmental friendliness, which support this technique to exhibit huge application prospects in the field of portable/wearable electronics, microelectromechanical system and human–machine interfacing.[11–14]

For the development of wearable electronics, the great efforts have been concentrated on pursuing the light weight and high flexibility, which can allow the devices to survive from various mechanical deformations and to be finally integrated on human skin.[15,16] Consequently, the design of the on-skin TENG device for powering wearable electronics is also experiencing several similar challenges. For example, the fabricated device is desired to possess both ultrathin thickness and high stretchability, which can cooperate with the mechanical motion of human skin and bring no change to the tension and elasticity of the skin. Meanwhile, the device should be able to firmly adhere to skin, while it can provide a good insulating performance for the electrification. For the TENG devices, the dielectric materials for electrification are easy to achieve high stretchability, while the conductive material for making the electrode is the key factor to restrain the stretchability of the whole device.[11,12,17] So far, the TENG with the highest stretchability is achieved by using ionic hydrogel and elastomer substrates, where the TENG can function stably under a strain over 1000%.[18] However, the thickness of hydrogel-based TENG cannot reach the ultrathin level and the overall thickness of the reported sample is around 2 mm, where the hydrogel electrode itself occupied more than 90% of the total thickness.[18] So far, the thinnest thickness of the similar hydrogel electrode that has been reported is around 100 μm,[19] which is still much larger than the thickness of the dielectric film used in the TENG device. Meanwhile, the viscosity of the hydrogel increases the complexity of assembly process for TENG devices, and the

Prof. X. Chen, Y. Wu, Dr. J. Shao, Dr. T. Jiang, Dr. A. Yu, Dr. L. Xu, Prof. Z. L. Wang
Beijing Institute of Nanoenergy and Nanosystems
Chinese Academy of Sciences
National Center for Nanoscience and Technology (NCNST)
Beijing 100083, China
E-mail: zlwang@gatech.edu
Prof. Z. L. Wang
CAS Center for Excellence in Nanoscience
National Center for Nanoscience and Technology (NCNST)
Beijing 100190, China
Prof. Z. L. Wang
School of Material Science and Engineering
Georgia Institute of Technology
Atlanta, GA 30332-0245, USA

DOI: 10.1002/smll.201702929

fine control of the shape of the hydrogel electrode is difficult to achieve. In this case, it is necessary to keep pursuing some simple and effective fabrication technique for an ultrathin and highly stretchable TENG device, which would be an ideal energy supplier for the wearable electronics.

On the basis of the above considerations, a highly stretchable TENG based on the ultrathin dielectric elastomers is proposed. The TENG device was using single-electrode mode, where the stretchable electrode made by carbon grease was sandwiched between two elastomer films. The total thickness of the device was about 102 μm, and the bottom surface of the device was super adhesive, which allowed the device to be stuck on various irregular surfaces. The open-circuit voltage (V_{oc}) and short-circuit current (I_{sc}) from the TENG with an effective contact area of 9 cm^2 can reach 115 V and 3 μA. The ultrathin thickness and the super flexibility of the device can even allow the device to work on human fingers without influencing the manual movement. Two kinds of sensory strategies have also been proposed, in order to reveal the application possibility of this elastic TENG in the field of wearable electronics system. Hence, this TENG device has the potential to serve as the second skin for human body, where the functions of energy collection or self-powered sensing can be realized without disturbing the daily behavior of the body.

2. Results and Discussion

Figure 1a showed the basic structure of this ultrathin TENG device and the photograph of the device attached on a human hand, while the energy generation from a TENG on human hand can be seen in Movie 1 in the Supporting Information. The TENG was using a single-electrode mode to collect energy from contact-separation motion, where the stretchable electrode was made by smearing the carbon/silicon grease on the surface of dielectric elastomers. A commercial VHB tape was selected as the dielectric elastomer and the grease electrode was sealed by two VHB films (3M, 9460). Figure 1b,c showed the

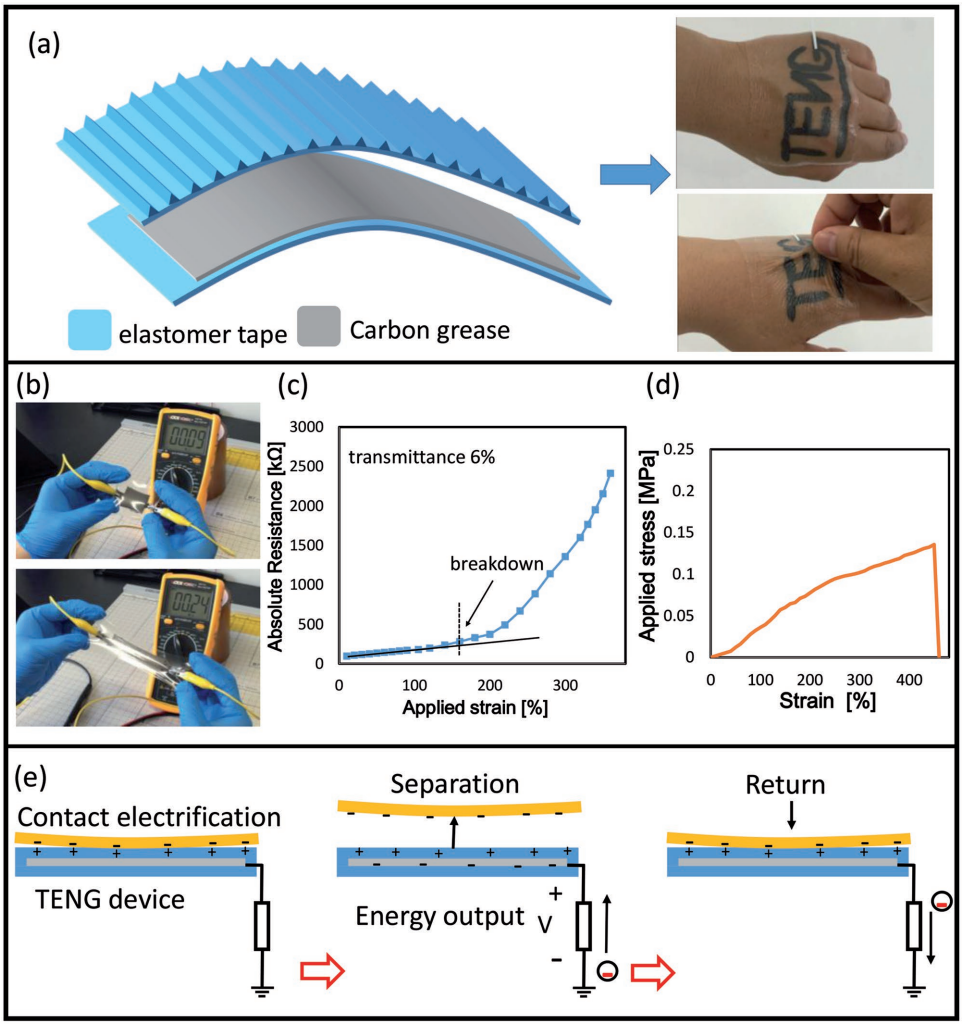

Figure 1. a) The basic structure of the elastic TENG and the photographs of the TENG attached to the human hand. b) Photographs of the resistance changing of the grease electrode. c) Summarized data about the resistance changing with different strains. d) Uniaxial tensile tests of the elastic TENG, where the final strain was 450%. e) The working mechanism of this elastic TENG, which is based on the single-electrode mode of the TENG device.

resistance changing of the grease electrode in response to different strains, where the unidirectional strain was applied on TENG sample with an electrode of 30 mm × 35 mm. The initial resistance of the electrode was around 90 kΩ (≈16 kΩ Y^{-1}). The increase of the resistance showed linear changing when the applied strain was smaller than 160%, which suggested that the decrease of the conductivity of the electrode was quite small and the increase of the resistance was mainly due to the change in geometry. When the applied strain was larger than the threshold value, the connection of the carbon grease would be broken and the resistance of the electrode would be increased dramatically (see Figure 1c). The micrograph of the grease electrode can be seen in Figure S1 in the Supporting Information. When the applied strain reached 400%, the grease electrode turned into a series of small islands, and the conductivity of the electrode was strongly decreased. In order to evaluate the mechanical properties of the TENG devices, the uniaxial tensile test was studied, as can be seen in Figure 1d. The ultimate stress of 0.132 MPa at a strain of 450% can be achieved for the TENG sample. We also found that the existence of the grease electrode brings almost no change to the stiffness of the elastomer film. Hence, both the ultrathin thickness and the high stretchability can be simultaneously achieved with our sample.

The working mechanism of the TENG relies on the coupling effect of triboelectric electrification and electrostatic induction, as schematically illustrated in Figure 1e. When an active object (such as glove, Kapton film, and even human skin) contacted with the elastomer film, the electrification process occurs on the contact interface. The same amount of charges with opposite polarities were generated at the surfaces of the moving object and the elastomer, respectively. The generated charge amount and polarity were determined by the electrification series of the two materials. In Figure 1e, we assumed that the active object was the dielectric material like Kapton film, which was more electrically negative in comparison with the elastomer film during the electrification process. Then, the separation motion between active object and the elastomer resulted in an accumulation of positive charges on the surface of the elastomer film (see Figure 1e). Accordingly, the potential drop between the surface of the elastomer film and the grounded position was established. Under the short-circuit condition, the electrons moved toward the grease electrode buried beneath the elastomer film to balance this potential drop and finally a strong electric field established across the elastomer film. Until the active object was quite far away, an electrical equilibrium achieved and the electrons stopped moving. When the active object returned to the contact position, the electrostatic field around the top surface of elastomer film was immediately neutralized by the negative charges on the active object. The electrons on the grease electrode moved back to the ground. During this whole motion cycle, two peak currents would be generated in the external circuit, and the energy output can be produced. Under the open-circuit condition, the same potential drop established between elastomer surface and the ground, while the electron motion cannot happen. A strong electric field can be detected between the grease electrode and the grounded position. The following contact motion of the active object led to the vanishing of this field. Hence, a square-wave voltage signal can be observed from TENG under the open-circuit condition. With the same triboelectric charge density, the generated output voltage was decided by the separation distance, while the output current dominated by the separation velocity.[20,21] In this case, the adhesive surface of the VHB film can suppress the output current, since its sticky characteristic can slow down the separation motion of the active object. Moreover, if the elastomer was strongly stuck to the active object, the separation motion may damage the TENG sample. Consequently, the top surface of the VHB elastomer needs to be modified for the triboelectrification process. Usually, people used inductively coupled plasma (ICP) reactive-ion etching technique to modify the surface of the dielectric film in TENG, and a high surface area can be achieved by covering the dielectric film with a series of nanopatterned structure. However, the detailed parameter setting for the ICP method required extensive experience and application of ICP method for larger area treatment sometimes met repeatability problems. In this study, we figured out a simple but effective method to modify the surface properties of the elastomer film, which can be an alternative for ICP method. **Figure 2**a showed the procedure of four steps treatment for printing nano/micropatterns on the surface of the elastomer film. First, the elastomer film was under UV–ozone treatment for 3 min. The UV–ozone treatment can solidify the surface of the elastomer and made it non sticky. After the treatment, the elastomer film was printed on the master plate with carved patterns. The elastomer film and the plate were placed in 80 °C oven for 1–2 min and then cooled down at −10 °C for 5 min. The cooling process can help to remove the master plate from elastomer. Finally, the elastomer with curved patterns can be achieved. In our experiments, we applied grating patterns on the surface of elastomer film, as can be seen in Figure 2b. The reflection effect of the grating pattern can be seen in Figure 2c and in Figure S2 (Supporting Information). The UV treatment strongly decreased the sticky characteristic of the elastomer film, which can accelerate the separation motion of the active object. The micrograting pattern can enhance the effective contact area between elastomer and the active objects. The similar modification method can also be applied as the transfer technique for elastic optical system, where the designed nanopattern or the optical matrix can be printed on the surface of elastomer film.

For the electrical measurement of the prepared TENG, two plates (top and bottom) were designed to be the moving objects, as explained later in the Experimental Section. The Kapton film was selected as the active object, and it was attached to the moving plate, which was guided by a linear motor in the vertical direction of the bottom plate. The prepared on-skin TENG was ultrathin and highly stretchable, and thus it had to be stick to some substrate for measurement. Otherwise, the TENG would automatically roll into a ball. As can be seen in **Figure 3**a, the thickness of the prepared elastic TENG is about 102 μm. The backside of the elastic TENG is super adhesive, and it can be attached to the surface of bottom plate (see Figure 3a). The top surface of the TENG was modified for contact electrification. Meanwhile, the grease electrode in TENG sample was a mesh structure instead of a square structure, and the detailed design of the grease electrode can be seen in Figure S3 (Supporting Information), where the effective contact region of the electrode is about 9 cm^2. The

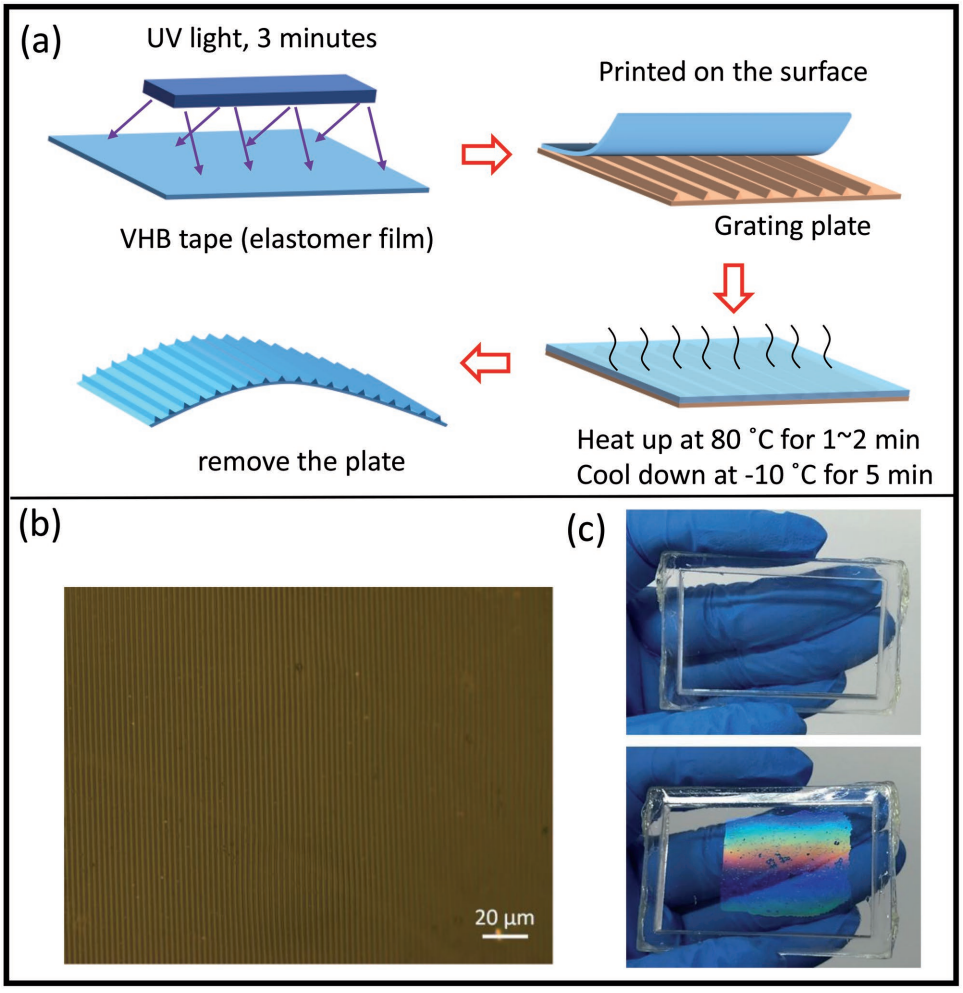

Figure 2. a) Surface modification process for treating the top surface of the TENG, where four steps treatment was applied to the sample. b) Micrograph of the printed grating pattern on the surface of the TENG. c) Photographs of the elastomer film after the modification and the light reflection effect can be seen on the modified surface.

mesh structure can help the elastomer film to firmly seal the grease electrode, which can finally increase the robustness of the TENG sample. At the beginning, two plates were aligned with each other, and the separation motion of the top plate with a position resolution of 1 mm can be guided by the linear motor. The separating movement was in a symmetric acceleration–deceleration mode with an acceleration rate of ±20 m s^{-2} and the motion velocity in our experiments is fixed to 1 m s^{-1}. The V_{oc} and I_{sc} were measured by an electrometer and the results can be seen in Figure 3b,c. The output energy within one motion cycle was mainly decided by the tribo-induced charges, while the resistance of the grease electrode can hardly change the output performance. The output characteristic with different external resistance has also been studied, as shown in Figure 3d. With the increase of the external resistance, the output current decreased from the I_{sc} to 0 and the output voltage increased from 0 to V_{oc}, which was the typical behavior of TENG device. The optimized external resistance for achieving the largest output power was around 60 MΩ. The output performance of the TENG showed no changing when the external resistance was smaller than 2 MΩ. This value was still more than 20 times larger than the resistance of the grease electrode, and thus the influences of the electrode resistance can be neglected. These results proved that carbon grease can be the ideal materials for the stretchable TENG. It can endure more 160% strains and offers almost no increase to the stiffness of the dielectric film. Meanwhile, its high resistive characteristic, which can be a huge defect for other electronics applications, is still in the acceptable range for the TENG devices.

The high stretchability was one of the major advantages of this elastic TENG, as discussed in Figure 1b,c. The viability of the output voltage of this TENG with the applied strain was further studied, as can be seen in Figure 3e. The TENG sample was uniaxially stretched to different strains (0–170%), and the average output voltage from the device was recorded by the electrometer. Here, the deformation of the TENG led to the change of the contact area. In order to rule out the influence from the area changing, the size of the Kapton film to contact with TENG was always kept to be the initial size of TENG. As can

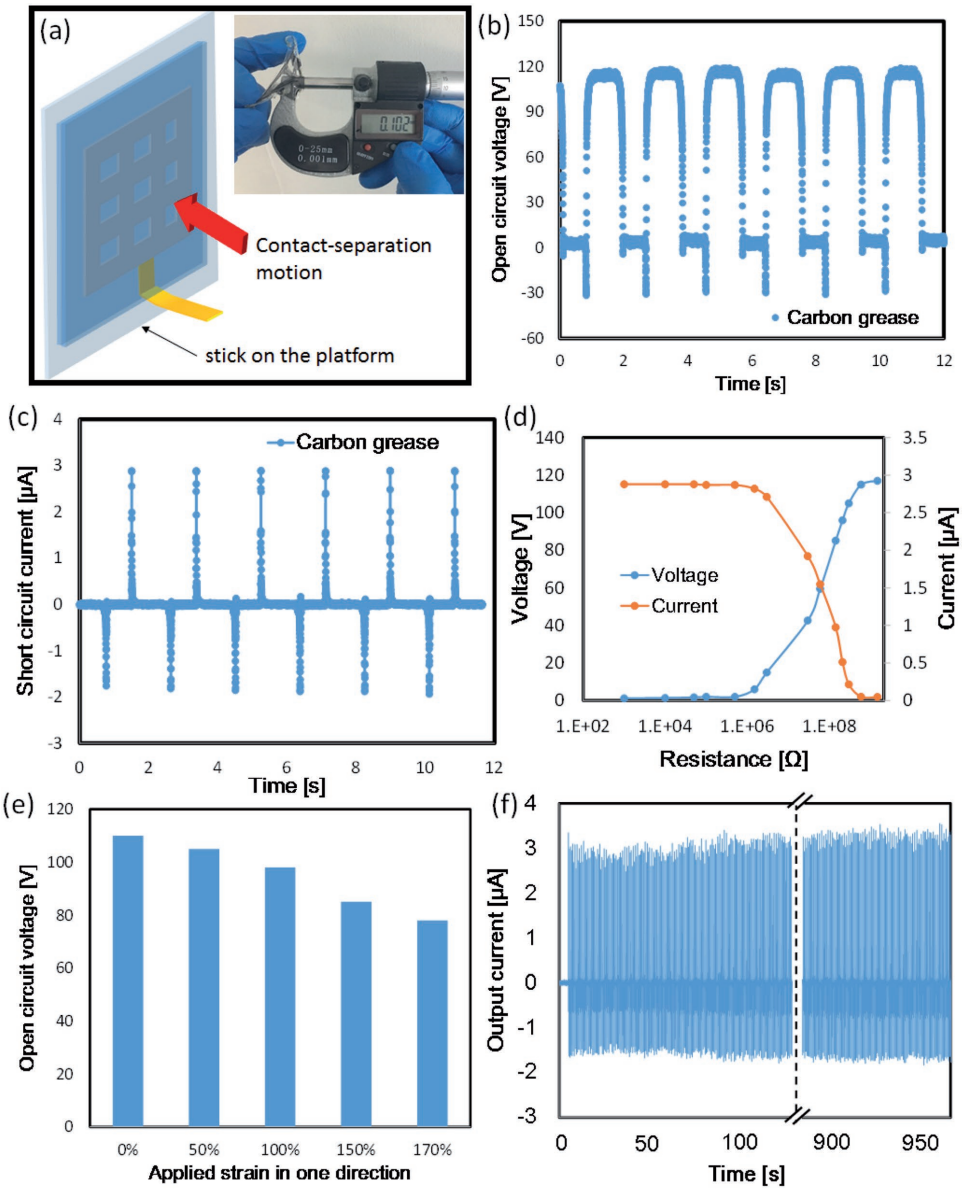

Figure 3. Performance measurement of the prepared TENG sample, a) the sample structure and the experimental system for the measurement, where the thickness of the TENG was measured to be 102 μm. b) The V_{oc} from TENG during contact-separation motion, c) The I_{sc} from TENG during contact-separation motion d) The output performance changing with the different external resistances. e) The V_{oc} from the TENG under different applied strains, where the size of the Kapton film for electrification was kept unchanged. f) I_{sc} from TENG that lasted for ≈2000 cycles of contact-separation motions.

be seen in Figure 3e, the increase of the applied strain resulted in the decrease of the output voltage. In Figure 1c, the resistance of the grease electrode under the strain of 200% was only 0.4 MΩ, which is still too small to change the output voltage from TENG. Hence, the charge-leakage phenomenon should account for the decrease of the output voltage. As explained in our previous studies, the insulating performance of the dielectric elastomer film is not as good as Kapton or PET films, and the leakage current through the elastomer can happen when the material is under high voltage.[22,23] The elastic TENG can work effectively with a strain of 170%, while the V_{oc} under this strain was decreased to be about 68 V. The durability of the elastic TENG was also performed over 2000 cycles. The repeated contact-separation motion has been continued for more than 16 min, as can be seen in Figure 3f. The I_{sc} shows no obvious degradation. We have prepared more ten samples for the repeatability test. Based on the empirical results, the elastic TENG can work very stably under an applied strain of 100%, and the thickness of the TENG at this strain is ≈50 μm. For the applied strain larger than 100%, the robustness of the elastomer film was gradually weakened and the durability of the sample also became unstable. The results showed that the samples under a strain larger than 170% had the high possibility to be broken within 500 motion cycles, while for

the sample under a strain of 100% could all survive from 2000 motion cycles.

In order to further exhibit the super flexibility of this elastic TENG, we attached the TENG on four fingers of a human hand, as shown in **Figure 4**a and the Movie 2 in Supporting Information. The elastic TENG can fully cooperate with the motion of human fingers, while it can generate energy by contacting with various materials (see Figure 4a). During the griping, squeezing, and clapping motion of human hand, people will feel almost no resistance from this elastic TENG, and the TENG can also function normally with all these different motions. When the elastomer contacted with different materials, the energy generation performance was changed due to the different electrification capabilities. We selected several common materials for testing the electrification capability, while the amplitude of the generated V_{oc} was recorded, as shown in Figure 4b. The Kapton film can induce the highest output voltage, while the electrification with PTFE film was very weak. It is important to note that the contact electrification is a complicated process that is dominated by several effects. Not only the material properties but also the mechanical effects, such as the surface roughness, stickiness, can all change the tribo-induced charges. Here, we recorded the experimental results of the electrification, and the detailed analysis about the activation factors is undergoing further studies. The multilayer structure of this elastic TENG has also been studied, in order to figure out the thickness dependence of the output performance. The V_{oc} and the maximum transferred charges (Q_{cs}) of the TENG sample with multilayer structure in contact with Kapton film were tested and summarized in Figure 4c,d. For the TENG with five layers elastomer film, the V_{oc} is decreased nearly 50% (see Figure 4c). Based on the results in Figure 3e, the leakage current through the elastomer film can decrease the V_{oc} value. Hence, we expected that the multilayer structure can suppress the leakage and the established V_{oc} may show slight increase with the double-layer sample. However, it is interesting to find that with the increase of the layer numbers both V_{oc} and Q_{sc} kept decreasing (see Figure 4c,d). Hence, it is quite possible that the ultrathin thickness may not be the cause of leakage current, and the leakage effect was mainly induced by the applied strain. The expansion of the elastomer film enlarged the localized defects and pinholes, which can exacerbate leakage current (see Figure 3e). This leakage phenomenon is one of the major challenges for this ultrathin elastic TENG.

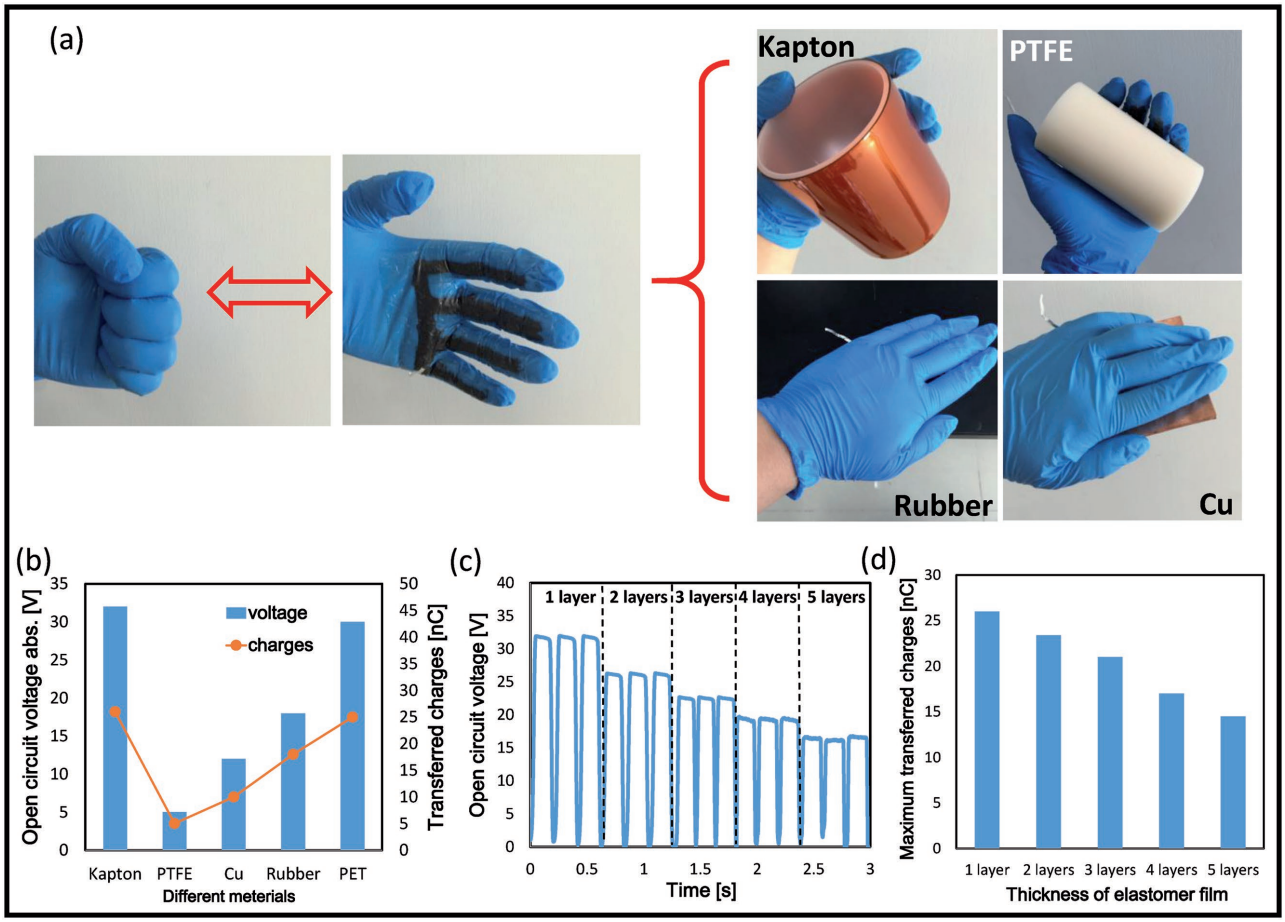

Figure 4. a) Demonstration of the super flexible performance of this on-skin TENG, where the TENG was attached to four fingers, and it can well function under the griping motion. b) Generated V_{oc} by using the TENG on fingers to gripe different materials. c) The summarized V_{oc} value of the multilayer sample in order to figure out the thickness dependence of the output performance, where the Kapton film is the active object for electrification. d) The change of Q_{sc} with increase the number of the elastomer layers.

If this elastic TENG was really attached to the human skin, the human body can induce a leakage path for the device and the energy generation efficiency may be suppressed. Hence, it is quite necessary to develop some new elastomer materials with better dielectric performance or with better surface morphology. It is important to note that common flexible dielectric materials with low stretchability are not able to fully cooperate with the skin motion and this is why the application of elastic material for TENG devices is quite necessary. As shown in Figure S4a and Video 3 in the Supporting Information, both the Kapton film and the elastomer film with the same thickness were attached to the human skin. During the squeezing motion of the hand, the Kapton film detached from the skin, while the elastomer film can smoothly work with the hand motion. Another advantage of this elastic TENG is the fine control during the electrode fabrication. The carbon grease can be painted on the elastomer film with the help of some curved mask, and we can precisely control the shape of the electrode. As can be seen in Figure S4b in the Supporting Information, a word "Tribo" with very fine font can be written on the human hand. In the real application, the electrode of this elastic TENG can be painted as some interesting tattoo on the skin, which makes the TENG device to be more attractive to the young people. Noteworthy that the elastic TENG is ultrathin and super flexible, which allow it to cooperate with various motions and deformations. Meanwhile, the backside of the device is highly adhesive, and thus it can be attached to the supporting objects with many irregular shapes. The universal applicability, biocompatibility, and the simple fabrication process ensured this elastic TENG to have great application potential in artificial muscle, electronics skins, and wearable/portable electronic systems.

To demonstrate this elastic TENG that can act as an active element for the self-powered sensing systems, we designed two kinds of sensory systems for detecting the touching position on the elastomer film. These two sensory systems have been delicately designed to utilize the advantages of this elastic TENG technique. The first sensory matrix was consisted of two groups of thin strip electrodes, as can be seen in **Figure 5**a. The grease electrode can be painted on the surface of elastomer film, and thus the fine control of the shape and the size of the electrode can easily be achieved. By utilizing this fabrication advantage, we designed a fine electrode network for sensory matrix and thus increased the resolution of the positioning system. As shown in Figure 5a, six strip electrodes with a width of 1 mm constructed a mesh network, and the space between two electrodes was 14 mm, which was the typical width of a human finger. The width of the electrode and the space can be adjusted for different touching objects. The sensory element consisted of three elastomer films, while the strip electrodes were divide into two groups (A, B, C and D, E, F) and were placed on two different layers, as illustrated in Figure 5a. The dielectric performance of the elastomer film can isolate two electrode groups and help to determine the position in vertical (A, B, C) and horizontal (D, E, F) directions, respectively. The working mechanism of this active sensor was similar to the energy generation process in the previous part. The contact-separation motion between the touching object and the elastomer film induced tribo charges on the surface of the elastomer film. Then, the grease electrodes sealed beneath the elastomer film can detect the established electrostatic field due to the induction effect. The touching object in the experiment was the human finger covered by Kapton tape. The key point of this sensory matrix was that each strip electrode can help to distinguish more than one position. The detailed strategy for the detecting process can also be seen in Figure 5b. There were typically three kinds of touching positions (see Figure 5b). That is, the crossover point of two electrodes, the position on only one electrode, and the empty region without electrode. We can distinguish all these three situations by comparing the output signal from the neighboring electrodes, as illustrated in Figure 5b. As can be seen in Figure S5 in the Supporting Information, when the touching position was gradually moving away from the strip electrode E, the output voltage from the electrode (channel E) decreased accordingly. In the real practice, the output signal from the TENG can be influenced by the touching stress and the variation of contact area. It is difficult to precisely refine the relationship between moving distance and the decrease of the output voltage. However, we can still recognize three kinds of touching positions, since the decreased range of the output voltage was quite significant for these three situations (see Figure S5, Supporting Information). Figure 5c–e showed three representative output signals from the sensory matrix. For the touching position at the crossover point of electrodes B and E, the two high output voltages (>10 V) can be detected from channels B and E, while the signals from all the other electrodes were all around 1.4 V (see Figure 5c). For the touching position on the electrode B only, the output voltage from electrode B was about 12 V, while the voltages from electrodes E and F were about 4 V (see Figure 5d). Hence, the touching position should be on the electrode D, while located between E and F. For the touching position on the empty region, the four electrodes (B, C, E, and F) that surrounded the touching position provided an output voltage around 4V (see Figure 5e). Then we can decide that the touching position was in the enclosed region of these four electrodes. Based on this identification strategy, a more accurate positioning process can be achieved by using the limited output electrodes. Each electrode in the matrix was an output channel and the six output channels were able to distinguish 25 touching positions. In the dense sensory matrix, with the increase of the sensor elements, the arrangement of the circuit pathway will become very complicated, which can finally restrain the minimum size of the sensory system. Hence, it is highly desirable to increase the accuracy of the sensor system without increasing the complexity of electrical connections. This proposed sensory strategy can provide more accurate positioning results with the same number of output channels, which can help to simplify the sensor system. Even though the identification of the output signal with different amplitudes may require a more complicated software program, it is still easier and cheaper than increasing the channel paths, especially for some complex sensory matrix.

Figure 6a showed a sensory system by using multilayer structure, which can serve as an alternative method to reduce the output channel of the sensory matrix. Four square electrodes were applied as a 2×2 matrix for detecting the touching position, while each electrode was placed on different elastomer

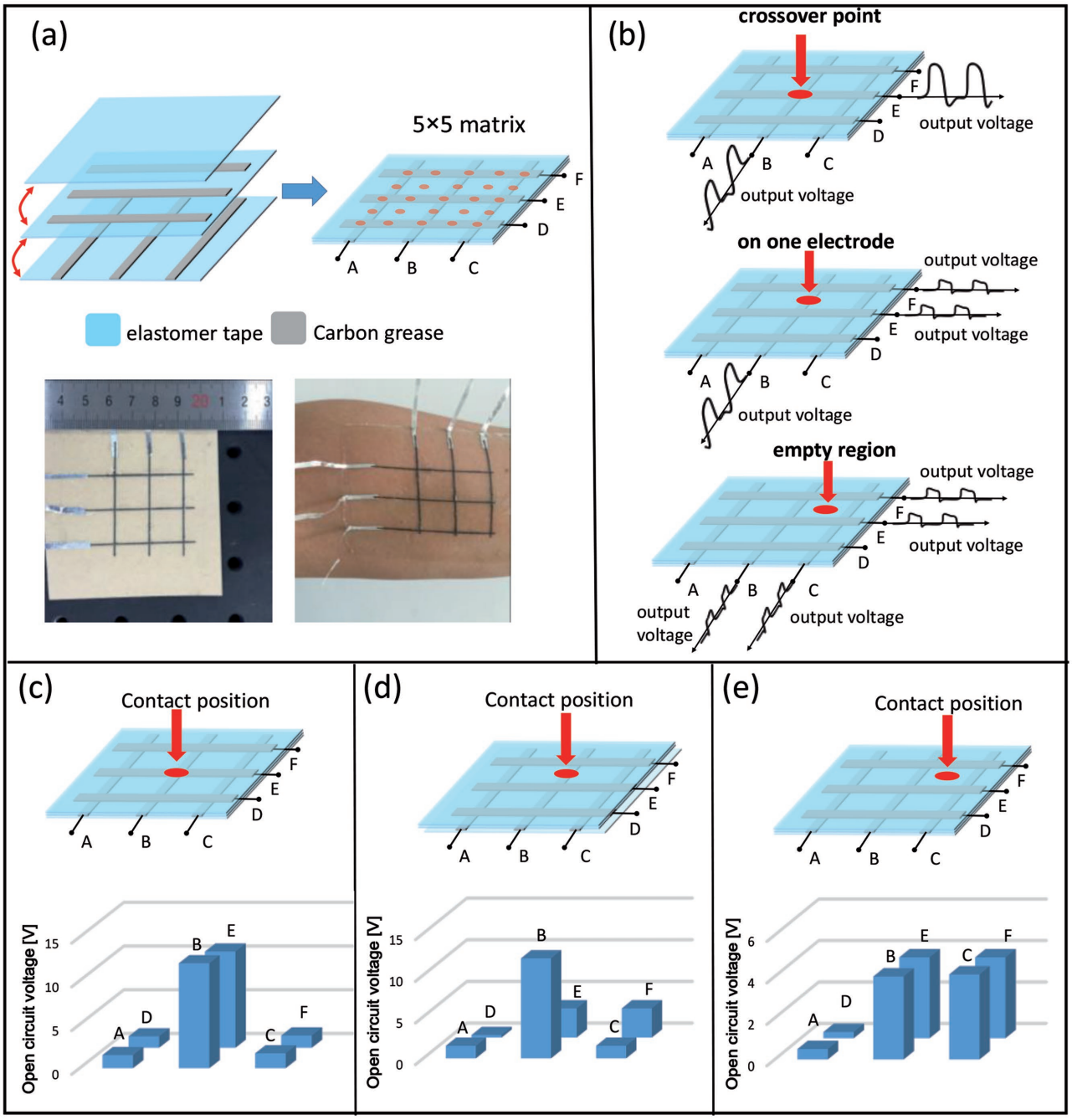

Figure 5. A touching sensor for detecting the contact position on the electronics skin by using the elastic TENG. a) The structure of the sensor matrix and the photographs of the sensor samples. b) A detailed strategy of the detection process. The sensor can distinguish three kinds of touching positions, the crossover point of two electrodes, the position on only one electrode and the empty region without electrode. The output voltage from the neighboring electrodes can be used to determine the three kinds of touching situations. c) The output voltage from the sensor matrix, when touching position was on the crossover point of electrodes B and E. d) The output voltage from the sensor matrix, when touching position was on the electrode B and in between electrodes E and F. e) The output voltage from the sensor matrix, when touching position was on the empty region.

layer (see Figure 6a). Four elastomer films were stacked together to form a multilayer sensory device and another elastomer film with modified surface covered on the top of the devices. The square electrode had a length of 5 mm and the distance between each electrode was 2.5 cm. The key point of this multilayer structure is to reduce the output channels for the sensory system. For the 2 × 2 matrix, only two output channels were enough to distinguish the four touching positions, as explained in Figure 6a. The electrodes A1 and A2 (B1 and B2) were connected to the output channel A (B), which means each

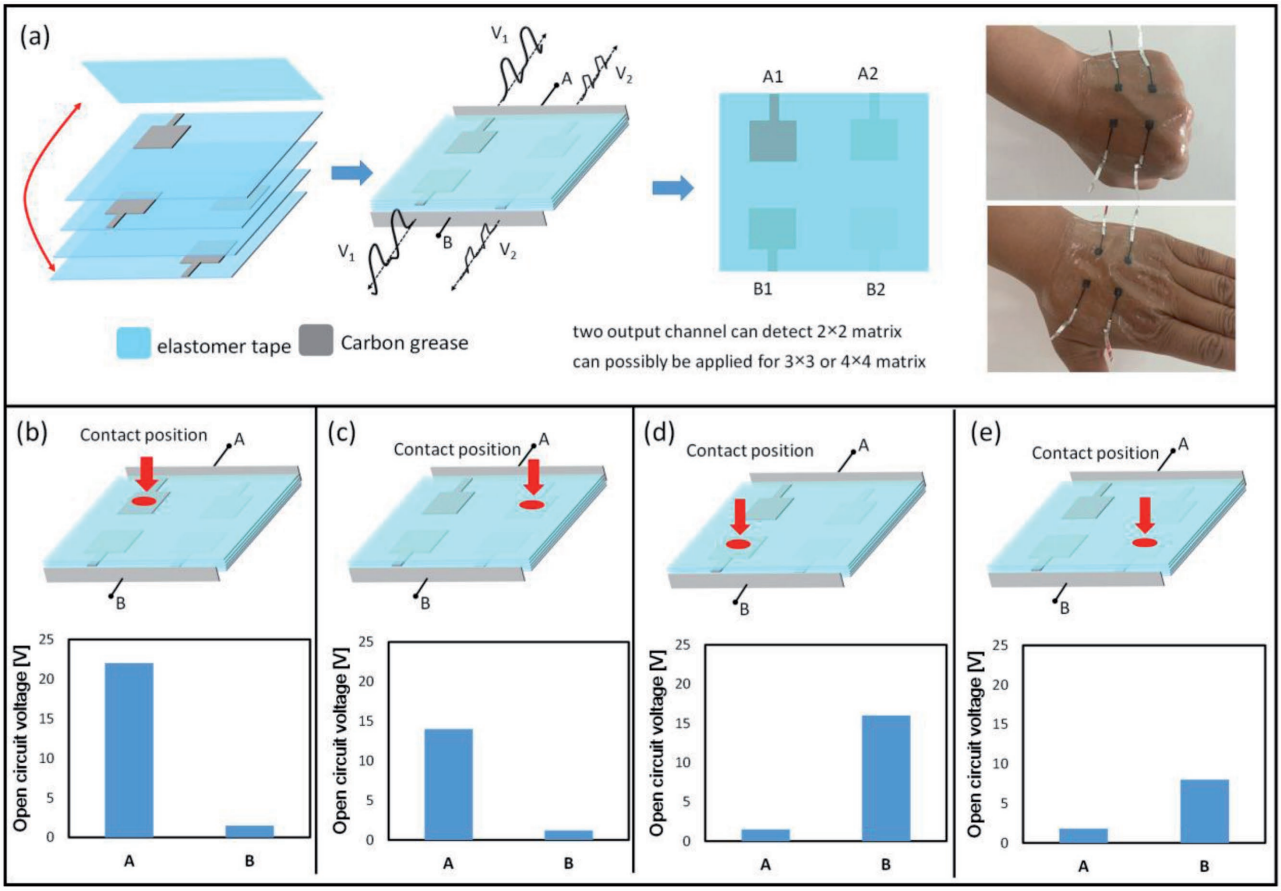

Figure 6. Another strategy for designing the sensor system by using multilayered structure. a) The structure of the sensor system. Four square electrodes were made by the carbon grease. The width of the electrode was around 5 mm and the space between two electrodes was around 25 mm. Each electrode was on a different layer and thus only two output channels were enough to distinguish the four touching positions. b) The output voltage from two channels, when the touching position is on electrode A1. c) The output voltage from two channels, when the touching position is on electrode A2. d) The output voltage from two channels, when the touching position is on electrode B1. e) The output voltage from two channels, when the touching position is on electrode B2.

output channel is responsible for revealing the signal from two electrodes. The two electrodes that connected to the same channel (A1–A2 or B1–B2) were separated by two elastomer films in the multilayer system (see Figure 6a). Accordingly, the output voltage from these two electrodes was changed due to the thickness difference. The output voltage from the two channels in response to four different touching positions can be seen in Figure 6b–e, respectively and the detailed output signals from each electrode under continuous touching motions were summarized in Figure S6a–d in the Supporting Information. The output signal from the two electrodes in one output channel can have an amplitude difference of 40%, which is enough for us to distinguish these two touching positions. The advantage of ultrathin thickness of this elastic TENG can be fully exploited in this sensor systems, which ensured that multilayer system still had a compact structure. For the five-layer system in Figure 6a, the total thickness of the device was still smaller than 0.5 mm. This multilayer system can reduce the output channels for the sensor matrix by delivering the output signal with different amplitude, which can simplify arrangement of the circuit pathway.

3. Conclusions

In summary, by utilizing the dielectric elastomer and the carbon grease electrodes, an ultrathin and highly stretchable TENG device is demonstrated. The total thickness of this elastic TENG is about 102 μm, and the device can work durably under a strain of 100%. The top surface of the device can be modified to have micrograting patterns by using a simple printing method, and the bottom surface of the device is super adhesive, which allows the device to attach to various supporting objects. The V_{oc} and I_{sc} from the device can reach 115 V and 3 μA, respectively, while the optimized external resistance of the device is 60 MΩ. The grease electrode in the device can endure a strain of 160%, and the fine design of the electrode can be easily achieved by using some curved masks, which suggests that carbon grease can be an ideal material for the stretchable TENG. Based on the unique feature of this elastic TENG, two kinds of self-powered sensor matrices have been designed, where the fine electrode shape and ultrathin thickness of the TENG can both be utilized to increase the accuracy of the sensor system. The proposed

elastic TENG has superior characteristics of ultrathin thickness, high stretchability, and fine controlled electrode geometry. Hence, this TENG device can serve as a fundamental element for the self-powered sensory system or as the energy supplier for the electronics skin, artificial muscles, and soft robotics, while it can also smoothly cooperate the daily motion of the body.

4. Experimental Section

Fabrication of Elastic TENG: The TENG device in this work was consisted of two stretchable dielectric elastomer films, and the soft electrode was sandwiched between two elastomer films. The dielectric elastomer (3M, 9460) had a thickness of 50 µm and could directly be applied for sealing the soft electrode. The soft electrode for TENG was based on conductive carbon/silicon grease (MG Chemicals). The electrode could be painted on the surface of the elastomer film, and the size and the shape of the electrode could be controlled by employing some curved mask. The bottom surface of the TENG device had the original adhesive nature of the elastomer film, while the top surface of the device was modified for contact electrification. The detailed modification process based on UV–ozone treatment can be seen in Figure 2a. The micropatterns could be printed on the top surface of the TENG, in order to enhance the electrification process. In this work, a commercial grating array was applied as the mater plate for printing process. The elastic TENG was ultrathin and super flexible. Hence, it had to be attached to the supporting objects for electrical measurements. The fabrication of sensor system was similar to the fabrication of the TENG, while the size and the location of the electrodes could be controlled by using mask.

Measurement of the TENG: The dielectric film for the electrical measurements was a Kapton adhesive tape (thickness ≈ 50 µm, 3 cm × 4 cm). The Kapton tape was fixed on a movable plate, and the plate was driven by a numerically controllable linear motor during the measurements. The sliding distance and the motion speeds could be controlled by the monitoring circuits. The generated voltage and current outputs were measured by Stanford Research Systems Kethiely 6514. The mechanical tensile test and stretch cycling test of the elastic TENG were performed by using an ESM301/Mark-10 system. For the tensile test, the strain rate was fixed at 50 mm min^{-1}.

Supporting Information

Supporting Information is available online from the Wiley Online Library or from the author.

Acknowledgements

This work was supported by the National Key R & D Project from Minister of Science and Technology (2016YFA0202704), the "thousands talents" program for pioneer researcher and his innovation team, China, NSFC Key Program (No. 21237003) and the National Natural Science Foundation of China (Grant Nos. 2016YFA0202704, 61405131, 51775049, 11674215, 5151101243, and 51561145021).

Conflict of Interest

The authors declare no conflict of interest.

Keywords

elastomer generators, electronics skin, triboelectric nanogenerators, wearable sensors

Received: August 25, 2017
Revised: September 6, 2017
Published online: October 23, 2017

[1] S. Lee, A. Reuveny, J. Reeder, S. Lee, H. Jin, Q. Liu, T. Yokota, T. Sekitani, T. Isoyama, Y. Abe, Z. Suo, T. Someya, *Nat. Nanotechnol.* **2016**, *11*, 472.
[2] J. Y. Oh, S. Rondeau-Gagné, Y. C. Chiu, A. Chortos, F. Lisse, G. J. N. Wang, B. C. Schroeder, T. Kurosawa, J. Lopez, T. Katsumata, J. Xu, C. Zhu, X. Gu, W. G. Bae, Y. Kim, L. Jin, J. W. Chung, J. B. H. Tok, Z. Bao, *Nature* **2016**, *539*, 411.
[3] T. Yamada, Y. Hayamizu, Y. Yamamoto, Y. Yomogida, A. Izadi-Najafabadi, D. N. Futaba, K. Hata, *Nat. Nanotechnol.* **2011**, *6*, 296.
[4] M. C. McAlpine, H. Ahmad, D. Wang, J. R. Heath, *Nat. Mater.* **2007**, *6*, 379.
[5] T. Sekitani, H. Nakajima, H. Maeda, T. Fukushima, T. Aida, K. Hata, T. Someya, *Nat. Mater.* **2009**, *8*, 494.
[6] J. Zhong, Q. Zhong, F. Fan, Y. Zhang, S. Wang, B. Hu, Z. L. Wang, J. Zhou, *Nano Energy* **2013**, *2*, 491.
[7] D. Yang, D. Kim, S. H. Ko, A. P. Pisano, Z. Li, I. Park, *Adv. Mater.* **2015**, *27*, 1207.
[8] Y. Mao, D. Geng, E. Liang, X. Wang, *Nano Energy* **2016**, *27*, 275
[9] S. K. Kima, R. Bhatiaa, T. Kima, D. Seo, J. H. Kim, H. Kim, W. Seung, Y. Kim, Y. H. Lee, S. W. Kim, *Nano Energy* **2016**, *22*, 483.
[10] X. Chen, Y. Song, Z. Su, H. Chen, X. Cheng, J. Zhang, M. Han, H. Zhang, *Nano Energy* **2017**, *38*, 43.
[11] X. Chen, X. Pu, T. Jiang, A. Yu, L. Xu, Z. L. Wang, *Adv. Funct. Mater.* **2017**, *27*, 1603788.
[12] X. Chen, T. Jiang, Y. Yao, L. Xu, Z. Zhao, Z. L. Wang, *Adv. Funct. Mater.* **2016**, *26*, 4906.
[13] L. Zheng, Y. Wu, X. Chen, A. Yu, L. Xu, Y. S. Liu, H. Li, Z. L. Wang, *Adv. Funct. Mater.* **2017**, *27*, 1606408.
[14] X. Chen, Y. Wu, A. Yu, L. Xu, L. Zheng, Y. Liu, H. Li, Z. L. Wang, *Nano Energy* **2017**, *38*, 91.
[15] M. Kaltenbrunner, S. Sekitani, J. Reeder, T. Yokota, K. Kuribara, T. Tokuhara, M. Drack, R. Schwödiauer, I. Graz, S. Bauer-Gogonea, S. Bauer, T. Someya, *Nature* **2013**, *499*, 458.
[16] M. Kaltenbrunner, M. S. White, E. D. Glowacki, T. Sekitani, T. Someya, N. S. Sariciftci, S. Bauer, *Nat. Commun.* **2012**, *3*, 770.
[17] S. Li, J. Wang, W. Peng, L. Lin, Y. Zi, S. Wang, G. Zhang, Z. L. Wang, *Adv. Energy Mater.* **2017**, *27*, 1602832.
[18] X. Pu, M. Liu, X. Chen, J. Sun, C. Du, Y. Zhang, J. Zhai, W. Hu, Z. L. Wang, *Sci. Adv.* **2017**, *3*, e1700015.
[19] C. Keplinger, J. Y. Sun, C. C. Foo, P. Rothemund, G. M. Whitesides, Z. Suo, *Science* **2013**, *341*, 984
[20] S. Niu, Y. Liu, X. Chen, S. Wang, Y. Zhou, L. Lin, Y. Xie, Z. L. Wang, *Nano Energy* **2015**, *12*, 760.
[21] L. Xu, Y. Pang, C. Zhang, T. Jiang, X. Chen, J. Luo, W. Tang, X. Cao, Z. L. Wang, *Nano Energy* **2017**, *31*, 351.
[22] X. Chen, T. Jiang, Z. L. Wang, *Appl. Phys. Lett.* **2017**, *110*, 033505.
[23] L. Maffli, S. Rosset, M. Ghilardi, F. Carpi, H. Shea, *Adv. Funct. Mater.* **2015**, *25*, 1656.

